EBioMedicine 27 (2018) 237–246

Contents lists available at ScienceDirect

EBioMedicine

journal homepage: www.ebiomedicine.com

Research Paper

Midkine Controls Arteriogenesis by Regulating the Bioavailability of Vascular Endothelial Growth Factor A and the Expression of Nitric Oxide Synthase 1 and 3

Thomas Lautz [a,b], Manuel Lasch [a,b], Julia Borgolte [a], Kerstin Troidl [c,d], Judith-Irina Pagel [a,e], Amelia Caballero-Martinez [a], Eike Christian Kleinert [a], Barbara Walzog [a,b], Elisabeth Deindl [a,b,*]

[a] Walter-Brendel-Centre of Experimental Medicine, University Hospital, LMU Munich, 81377 Munich, Germany
[b] Biomedical Center, LMU Munich, 81377 Munich, Germany
[c] Department of Vascular and Endovascular Surgery, Goethe-University-Hospital, 60590 Frankfurt am Main, Germany
[d] Division of Arteriogenesis Research, Max Planck Institute for Heart and Lung Research, 61231 Bad Nauheim, Germany
[e] Hospital of the University of Munich, Department of Anesthesiology, LMU Munich, 81377 Munich, Germany

ARTICLE INFO

Article history:
Received 11 August 2017
Received in revised form 21 November 2017
Accepted 21 November 2017
Available online 26 November 2017

Keywords:
Midkine
Arteriogenesis
Vascular endothelial growth factor A
Vascular endothelial growth factor receptor 2
Endothelial nitric oxide synthase
Neuronal nitric oxide synthase

ABSTRACT

Midkine is a pleiotropic factor, which is involved in angiogenesis. However, its mode of action in this process is still ill defined. The function of midkine in arteriogenesis, the growth of natural bypasses from pre-existing collateral arteries, compensating for the loss of an occluded artery has never been investigated. Arteriogenesis is an inflammatory process, which relies on the proliferation of endothelial cells and smooth muscle cells. We show that midkine deficiency strikingly interferes with the proliferation of endothelial cells in arteriogenesis, thereby interfering with the process of collateral artery growth. We identified midkine to be responsible for increased plasma levels of vascular endothelial growth factor A (VEGFA), necessary and sufficient to promote endothelial cell proliferation in growing collaterals. Mechanistically, we demonstrate that leukocyte domiciled midkine mediates increased plasma levels of VEGFA relevant for upregulation of endothelial nitric oxide synthase 1 and 3, necessary for proper endothelial cell proliferation, and that non-leukocyte domiciled midkine additionally improves vasodilation.

The data provided on the role of midkine in endothelial proliferation are likely to be relevant for both, the process of arteriogenesis and angiogenesis. Moreover, our data might help to estimate the therapeutic effect of clinically applied VEGFA in patients with vascular occlusive diseases.

1. Introduction

Vascular occlusive disease such as myocardial infarction, stroke or peripheral artery diseases are still a major cause of morbidity and mortality worldwide. Searching for new, non-invasive options to treat affected patients, much effort is made to understand the molecular mechanisms of arteriogenesis. Arteriogenesis is a tissue- and even life-saving process and presents the growth of pre-existing collateral arterioles to natural biological bypasses. It is provoked by increased fluid shear stress and is mediated by sterile inflammation (Chillo et al., 2016).

Midkine (MK) is a retinoic acid inducible cytokine, which is highly expressed during embryogenesis (Kadomatsu et al., 1990). In the adulthood its expression is restricted to certain tissues but strongly induced during inflammatory processes (Badila et al., 2015) such as rheumatoid arthritis, inflammatory bowel disease, and multiple sclerosis (for an overview see (Weckbach et al., 2011)), which are associated with angiogenesis. MK has also been implicated in angiogenesis and hence endothelial cell (EC) proliferation under conditions of tissue ischemia (Weckbach et al., 2012) and tumor growth (Choudhuri et al., 1997; Muramaki et al., 2003) as well as in neointima formation (Hayashi et al., 2005; Horiba et al., 2000). The functional role of MK in angiogenesis is still not well defined, however, it was shown that MK induces chemotaxis of neutrophils and supports neutrophil adhesion during inflammation (Takada et al., 1997; Weckbach et al., 2014). Neutrophils themselves express high levels of MK, but do not release it (Weckbach et al., 2012; Weckbach et al., 2014; Narita et al., 2008). However, after stimulation with the chemokine (C-X-C) ligand 1 (CXCL1) neutrophils release angiogenic growth factor such as vascular endothelial growth factor A (VEGFA) (Scapini et al., 2004).

The functional role of MK in arteriogenesis has never been investigated. Moreover, the functional role of VEGFA in arteriogenesis is controversially discussed (Jazwa et al., 2016). In vitro data from Tzima et al., who

* Corresponding author at: Walter-Brendel-Centre of Experimental Medicine, Marchioninistr. 15, 81377 Munich, Germany.
E-mail address: Elisabeth.Deindl@med.uni-muenchen.de (E. Deindl).

https://doi.org/10.1016/j.ebiom.2017.11.020

identified the VEGF receptor 2 (VEGFR-2), to be part of a mechanosensory complex and to be relevant for phosphoinositide 3-kinase (PI3K) activation, even suggested that VEGFR-2 is ligand-independent activated in response to shear stress (Tzima et al., 2005). Here, we demonstrate that leukocyte domiciled midkine controls the plasma bioavailability of VEGFA, which in turn is relevant for the expression of neuronal nitric oxide synthase (*Nos1*) and endothelial *Nos* (*Nos3*) (but not inducible *Nos* (*Nos2*)) in endothelial cells of collaterals. For arteriogenesis all three isoform of NOS, namely NOS1, NOS2 and NOS3 are described to be involved, although the function of the individual NOS is not well defined (Troidl et al., 2010; Pagel et al., 2011). Exclusively for NOS3 it has been shown that it mediates vasodilation in growing collaterals (Troidl et al., 2010). Here we show that *Nos1* or *Nos3* expression, respectively, is essential for collateral endothelial cell proliferation, whereby both isoforms are likely to be able to substitute for each other.

Collectively, our data provide mechanistic insights into MK-mediated endothelial cell proliferation, which are likely to be relevant not only for the process of arteriogenesis, but also for other inflammatory processes as well as tumor growth being associated with angiogenesis and hence endothelial cell proliferation.

2. Materials and Methods

2.1. Animals and Treatments

All experiments were carried out according to the German animal legislation guidelines and were approved by the Bavarian Animal Care and Use Committee. Mice were kept under a 12-hour (h) day and night cycle with chow and water provided ad libitum.

Mice were treated with either 100 μl DETA NONOate (Cayman Chemical, Ann Arbor, MI) 0.12 mg/ml intraperitoneal once daily in 0.9% NaCl (saline) (Braun, Melsungen, Germany), with 50 μl recombinant murine midkine (rmMK) (PeproTech, Rocky Hill, NJ) 0.1 mg/ml subcutaneously twice daily in saline or with 100 μl recombinant murine VEGFA164 (rmVEGFA) (Sigma-Aldrich, St. Louis, MO) 0.01 mg/ml intraperitoneal once daily in saline. Control groups received saline only. Sodium nitrite (Sigma-Aldrich) was applied via drinking water at a concentration of 1 g/l (Kumar et al., 2008; Hannas et al., 2010). Control groups received normal drinking water. Treatment was started 3 days (d) before the surgical procedure and continued until the end of the experiments.

2.2. Femoral Artery Ligation, Laser Doppler Imaging and Bone Marrow Transplantation

Collateral artery growth was investigated in a murine hindlimb model (Chillo et al., 2016) using 8- to 10-week-old male *Mdk*$^{-/-}$ (carrying the *Mdk*^{tm1Tmu} allele, RRID: MGI:3579532) (Nakamura et al., 1998), *Nos1*$^{-/-}$ (B6.129S4-*Nos1*^{tm1Plh}/J, RRID: IMSR_JAX:002986) (Huang et al., 1993) mice and appropriate WT controls (C57BL/6J mice, RRID: IMSR_JAX:000664; Charles River, Sulzfeld, Germany). Mice underwent ligation of the right femoral artery distally to the origin of the profunda femoris branch using a 7-0 silk braided suture (Peasalls Sutures, Somerset, Great Britain). During the surgical procedures mice were under general anesthesia with a combination of fentanyl (0.05 mg/kg body weight) (Janssen-Cilag, Neuss, Germany), midazolam (5.0 mg/kg body weight) (Ratiopharm, Ulm, Germany) and medetomidine (0.5 mg/kg body weight) (Pfizer, New York, NY), which was administered subcutaneously. The left leg underwent sham operation and was used as control. Perfusion of the paws was assessed using a LDI technique (Moor LDI 5061 and Moor Software Version 3.01, Moor Instruments, Remagen, Germany) under temperature-controlled conditions. The measurements were conducted before FAL (basal), immediately after FAL (aFAL), 3d and 7d after FAL. Color-coded images of the paws representing the flux value were used to calculate the ratio of the tissue perfusion of the occluded (Occ) to the Sham-operated (Sham) paw. For bone marrow transplantation see the Supplemental Experimental Procedures.

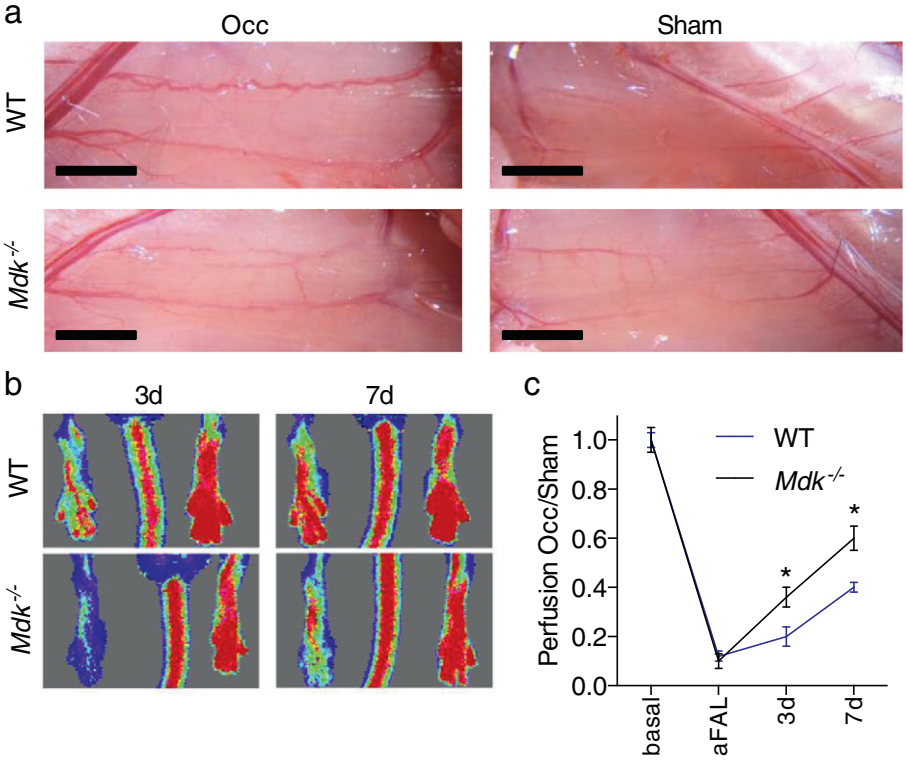

Fig. 1. *Mdk*$^{-/-}$ mice show reduced perfusion recovery after FAL. (a) Representative images of superficial collateral arteries in the adductor muscles of WT (upper panels) and *Mdk*$^{-/-}$ (lower panels) mice 7d after FAL (Occ) or sham operation (Sham). Scale bars: 3 mm. (b) Representative LDI images of WT (upper panel) and *Mdk*$^{-/-}$ (lower panel) mice 3d and 7d after FAL. (c) Line graph displaying the perfusion ratio (Occ/Sham) of WT and *Mdk*$^{-/-}$ mice before FAL (basal), immediately after FAL (aFAL), 3d and 7d after FAL. $n = 5$. *P < 0.05 WT compared with *Mdk*$^{-/-}$, two-way ANOVA with Bonferroni's multiple comparison test. Data shown are means ± SD.

2.3. Tissue and Blood Sampling

Heparinized blood gained by cardiac puncture was centrifuged (2.300*g* at 4 °C for 20 min) and plasma was stored at −80 °C. Prior to harvesting superficial collateral arteries for qRT-PCR (quantitative real-time PCR), both hind limbs were perfused with latex flexible compound (Chicago Latex, Chicago, IL) via a catheter in the abdominal aorta. For each mouse two superficial collateral arteries per side were isolated, snap frozen in dry ice and stored at −80 °C until further investigations.

For histological analysis of collateral arteries, mice were perfused with 20 ml adenosine buffer (1% adenosine (Sigma-Aldrich), 5% bovine serum albumin (BSA, Sigma-Aldrich) dissolved in phosphate buffered saline (PBS, PAN Biotech, Aidenbach, Germany), pH 7.4), to assure maximum vasodilatation (Chillo et al., 2016), followed by 20 ml 4% paraformaldehyde (PFA, Merck, Darmstadt, Germany) (for paraffin embedding) or 20 ml 3% PFA (for cryopreservation) in PBS, pH 7.4.

For histological analysis adductor muscles were rinsed in 4%PFA for 24 h and after paraffin embedding cut in 4 μm cross-sections. For immunofluorescence staining the samples were placed in 15% sucrose (Sigma-Aldrich), dissolved in PBS, for 4 h, followed by 30% sucrose, dissolved in PBS, overnight at 4 °C. Afterwards the adductor muscle tissue was cryopreserved in tissue tek (Sakura, Alphen aan den Rijn, The Netherlands) and cut in 6 μm cross-sections.

2.4. Histology and Immuno-Histology

Paraffin embedded cross-sections were stained with GIEMSA according to standard procedures. The number of collaterals on the Occ and Sham side of WT and *Mdk*$^{-/-}$ mice was counted 7d after FAL with an Axioskop 40 microscope and Axiocam 105 color (Carl Zeiss AG, Feldbach, Switzerland). On the Occ side only collaterals with a luminal diameter larger than 25 μm were defined as growing collaterals. Collaterals with a smaller diameter were not analyzed in the following investigations, since their diameter was comparable to the diameter of collaterals on the Sham side and hence didn't grow after FAL (Fig. S1). Luminal diameter and vascular wall of collateral arteries were analyzed with AxioVs40 V4.8.2.0 software (Carl Zeiss AG). For each mouse 5 slices with 3 growing collaterals on each slice were measured.

Mice were treated daily with 100 μl bromodeoxyuridine (BrdU) (BD Biosciences, San Jose, CA) (12.5 mg/ml dissolved in PBS, intraperitoneal) starting at the day of the surgical procedure. A standardized BrdU In-Situ Detection Kit (BD Biosciences) was used to analyze the proliferation of ECs and SMCs in collateral arteries 7d after FAL. For immunofluorescence staining 24 h after FAL, cryofixed tissue sections were stained with combinations of the following antibodies: primary anti-MK antibody (Cat#: PA5-19640, RRID: AB_10985009, Thermo Fischer Scientific, Waltham, MA, dilution 1:100, for 12 h at 4 °C), or primary anti-

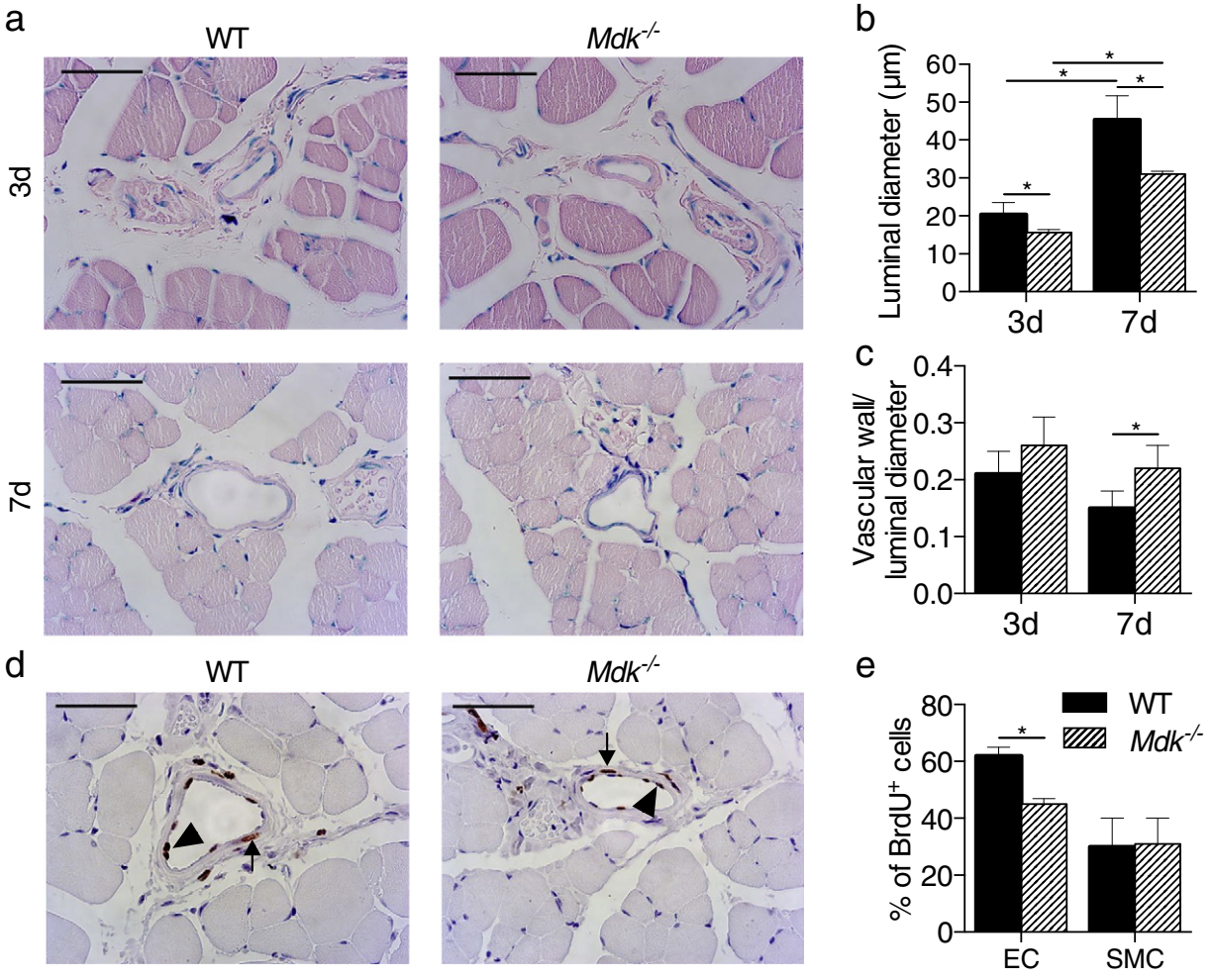

Fig. 2. Collateral vessel morphology after FAL. (a) Representative pictures of Giemsa stained slices showing collaterals in the adductor muscle of WT (left) and *Mdk*$^{-/-}$ mice (right) 3d (upper panel) and 7d (lower panel) after FAL. Scale bars: 50 μm. Bar graphs representing (b) the luminal diameter and (c) the ratio of the vascular wall to the luminal diameter of WT and *Mdk*$^{-/-}$ collaterals 3d and 7d after FAL. 5 slices with 3 collaterals per slice were analyzed per mouse and time point. (d) Representative pictures of BrdU stained tissue sections with BrdU^{+} ECs (arrowhead) and BrdU^{+} SMCs (arrow) 7d after FAL. (e) Bar graph displaying the percentage of BrdU^{+} and hence proliferated ECs and SMCs in WT and *Mdk*$^{-/-}$ collaterals 7d after FAL. 3 slices with 3 collaterals each were analyzed per mouse. $n = 5$. *$P < 0.05$, one-way ANOVA with Bonferroni's multiple comparison test (b, c) or unpaired Student's *t*-test (e). Data are means ± SD.

VEGFA164 antibody (Cat#: AF-493-SP, RRID: AB_354506, Novus Biological, Littleton, CO, dilution 1:50, for 12 h at 4 °C), secondary donkey anti-rabbit antibody (Cat#: A10040, RRID: AB_2534016, Thermo Fischer Scientific, dilution 1:200, for 1 h at room temperature), anti-Ly-6G antibody (Cat#: ab25024, RRID: AB_470400, Abcam, Cambridge, MA, dilution 1:100, for 12 h at 4 °C) and DAPI (Cat#: D1306, RRID: AB_2629482, Thermo Fischer Scientific, dilution 1:1000, for 20 min at room temperature). Cross-sections were covered with Mowiol (Sigma-Aldrich) and analyzed with a confocal microscope (Leica SP5, Leica, Wetzlar Germany).

2.5. Protein Levels of VEGFA and MK

The VEGFA plasma level was measured with a standardized ELISA Kit (R&D Systems, Minneapolis, MN) following the manufacturer's protocol. The ready-SET-go Midkine ELISA-Kit (USCN Life Science Inc., Wuhan, China) was used to measure the MK plasma level following the manufacturer's protocol.

2.6. RNA Isolation, cDNA Synthesis and qRT-PCR

After isolating RNA from collateral arteries or primary endothelial cells with Trizol (Life technologies, Carlsbad, CA), RQ1 RNase-Free DNase (Promega, Madison, WI) digestion was used to remove residual genomic DNA. 250 ng purified RNA (using RNeasy MinElute columns (Qiagen, Hilden, Germany)) was reverse transcribed into cDNA with the QuantiTect Rev. Transcription Kit (Qiagen). For qRT-PCR analysis the SYBR Power Green Kit (Life Technologies) was used according to the manufacturer's protocol with 1 μl of the 1:5 diluted cDNA and 0.5 μM of each primer per reaction. For further information see the Supplemental Experimental Procedures.

2.7. Cell Culture

Mouse aortic ECs and SMCs were isolated as previously described (Kobayashi et al., 2005). In brief, isolated murine aortas were filled with collagenase type II (Biochrom AG, Berlin, Germany) solution (2 mg/ml, dissolved in serum-free Dulbecco's Modified Eagle's Medium (DMEM, Sigma-Aldrich)) for 45 min at 37 °C, and afterwards the ECs were flushed out of the aortas with DMEM containing 20% fetal calf serum (FCS, PAN Biotech). ECs were cultured with Complete Mouse Endothelial Cell Medium (Cellbiologics, Chicago, IL) on collagen A (Biochrom AG) coated flasks. The remaining aorta was cut into 2 mm pieces and placed on a 1% gelatin-coated dish (PAN Biotech). After 10 days the tissue pieces were removed and SMCs were cultured with Complete Mouse Smooth Muscle Cell Medium (Cellbiologics) on 1%

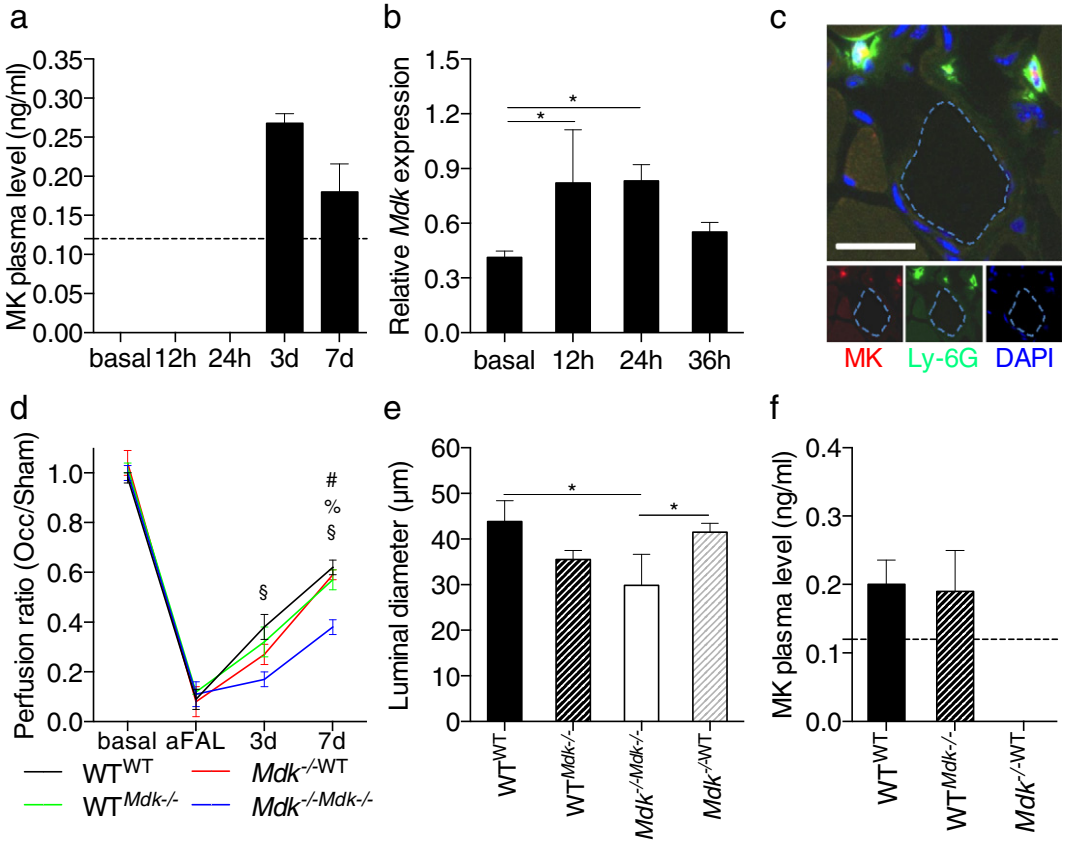

Fig. 3. Bone marrow cell delivered MK is essential for collateral artery growth. (a) Bar graph displaying the plasma level of MK (ng/ml) in WT mice prior to any surgical procedure (basal), 12 h, 24 h, 3d and 7d after FAL. Dashed line shows the detection limit of the ELISA kit (0.128 ng/ml). $n = 5$ in triplicates. (b) Bar graph representing the expression level of *Mdk* mRNA in collaterals of WT mice prior to any surgical procedure (basal), 12 h, 24 h and 36 h after FAL as quantified by qRT-PCR. Data were normalized to the expression level of the 18S rRNA. $n = 5$ in triplicates. *P < 0.05, one-way ANOVA with Bonferroni's multiple comparison test. (c) Immunofluorescence staining for MK (red, lower panel, left), neutrophils (Ly-6G, green, lower panel, middle) and nuclei (DAPI, blue, lower panel, right) 24 h after FAL. Ly-6G$^+$ cells in perivascular tissue stained positive for MK (upper panel). Blue dotted lines indicate the endothelial layer of the collateral artery. Scale bar: 25 μm. (d) Line graph displaying the perfusion ratio (Occ/Sham) as measured by LDI in bone marrow transplanted mice before FAL (basal), immediately (aFAL), 3d and 7d after FAL. For the bone marrow transplant studies WT mice received $Mdk^{-/-}$ donor bone marrow ($WT^{Mdk-/-}$) and vice versa ($Mdk^{-/-WT}$). WT^{WT} and $Mdk^{-/-\ Mdk-/-}$ transplanted mice were used as control groups. $n = 4$ per group. $^{§}P < 0.05$ (WT^{WT} compared with $Mdk^{-/-\ Mdk-/-}$), $^{\#}P < 0.05$ ($Mdk^{-/-\ WT}$ compared with $Mdk^{-/-\ Mdk-/-}$), $^{\%}P < 0.05$ ($WT^{Mdk-/-}$ compared with $Mdk^{-/-\ Mdk-/-}$), two-way ANOVA with Bonferroni's multiple comparison test. (e) Bar graph representing the luminal diameter of collaterals in bone marrow transplanted mice 7d after FAL. $n = 4$. 5 slices with 3 collaterals each were analyzed per mouse. *P < 0.05, one-way ANOVA with Bonferroni's multiple comparison test. (f) Bar graph displaying the MK plasma level (ng/ml) in bone marrow transplanted mice 7d after FAL. The dashed line shows the detection limit of the ELISA kit (0.128 ng/ml). $n = 4$. Data shown are means ± SD.

gelatine coated flasks. Medium was changed every other day and passages 1 to 3 were used for experiments.

2.8. In Vitro BrdU Proliferation Assays

A 96-well plate with 1.2×10^4 ECs or SMCs per well and a standardized BrdU proliferation kit (Roche, Basel, Switzerland) was used to analyze the in vitro proliferation of isolated ECs or SMCs. For further information see the Supplemental Experimental Procedures.

2.9. Statistical Analysis

Experimenters were blind to outcome assessment for all experiments. All statistical analysis were performed with GraphPad software PRISM6 (GraphPad Software, La Jolla, CA) and are specified in the Figure legends. Data shown are means ± SD. Results were considered to be statistically significant at $P < 0.05$.

3. Results

3.1. Midkine Is Essential for EC Proliferation of Growing Collateral Arteries

To characterize the functional role of MK in arteriogenesis, we investigated a murine hindlimb model in which femoral artery ligation (FAL, Occ) results in collateral artery growth (Chillo et al., 2016). Our data showed that FAL results in a reduced increase in caliber size and tortuosity of superficial collateral arteries as well as a significantly reduced perfusion recovery in *Mdk* deficient ($Mdk^{-/-}$) compared to wild-type (WT) mice (Fig. 1a–c). To investigate whether the reduced perfusion recovery observed in $Mdk^{-/-}$ mice was due to a reduced number of preexisting arteriolar connections, we performed histological analyses. Our results revealed identical numbers of collaterals with increased luminal diameter (3 per slice per mouse) as well as total numbers of all collaterals (Occ = 5, Sham = 5, per slice per mouse) in WT and $Mdk^{-/-}$ mice (Fig. S1). Moreover, the luminal diameters of collateral arteries of the Sham side were comparable in WT and $Mdk^{-/-}$ mice (Figs. S1 and S2). However, compared to WT mice, $Mdk^{-/-}$ mice showed a

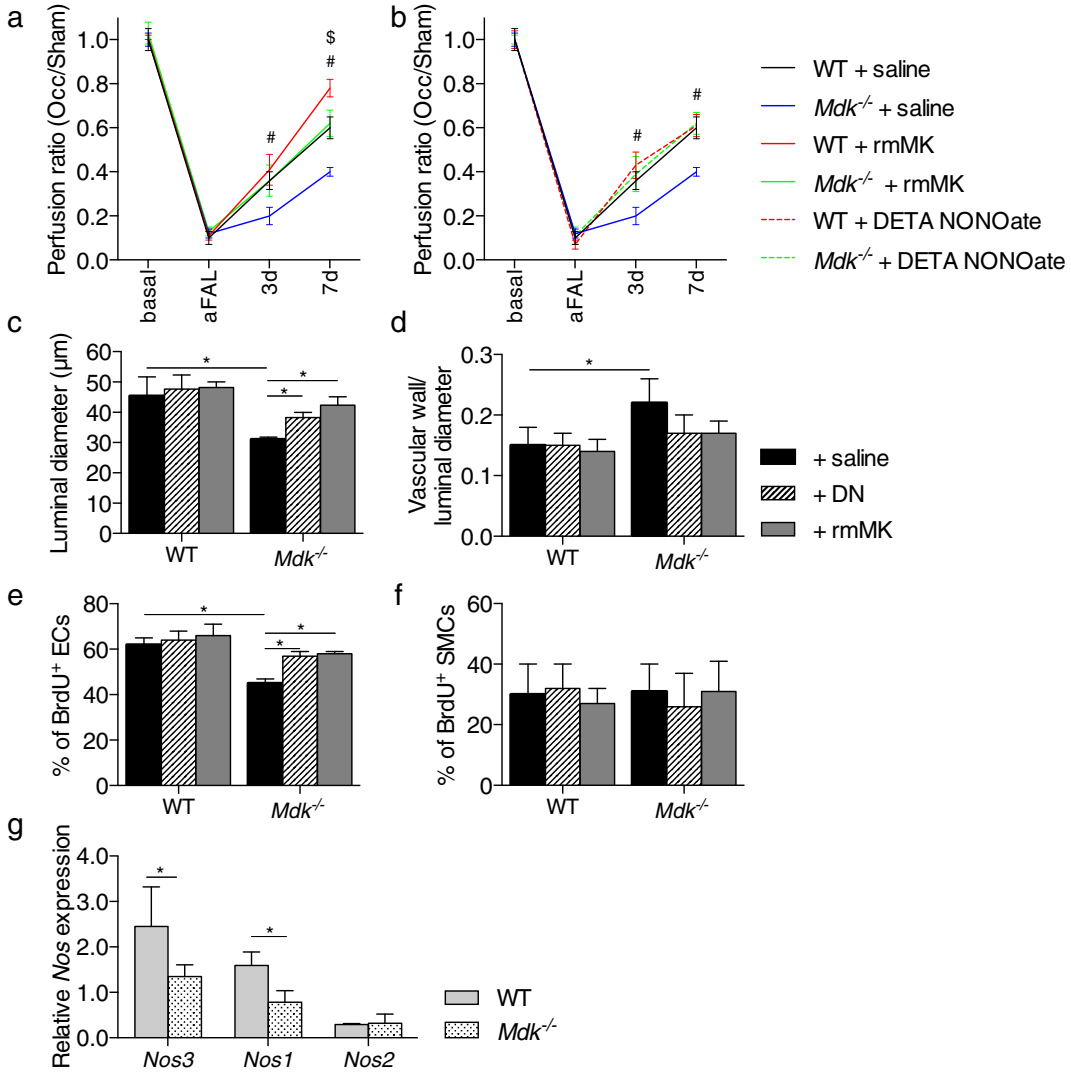

Fig. 4. Treatment with DETA NONOate as well as with rmMK rescues arteriogenesis in $Mdk^{-/-}$ mice. Line graphs displaying the perfusion ratio (Occ/Sham) as measured by LDI in WT and $Mdk^{-/-}$ mice after treatment with saline, rmMK (a), or DETA NONOate (b), respectively. $n = 5$. $^{\#}P < 0.05$ (compared with $Mdk^{-/-}$), $^{\$}P < 0.05$ (WT + rmMK compared with WT + saline and compared with $Mdk^{-/-}$), two-way ANOVA with Bonferroni's multiple comparison test. Bar graphs displaying the luminal diameter (c) and the ratio of the vascular wall to the luminal diameter (d) of WT and M $Mdk^{-/-\ Mdk-/-}$, collaterals 7d after FAL. 5 slices with 3 collaterals each were analyzed per mouse. Bar graphs displaying the percentage of $BrdU^+$ ECs (e) and SMCs (f) in WT and $Mdk^{-/-}$ collaterals 7d after FAL. 3 slices with 3 collaterals each were analyzed per mouse. $n = 5$. $^*P < 0.05$, one-way ANOVA with Bonferroni's multiple comparison test. (g) Bar graph representing the expression level of *Nos1*, *Nos2* and *Nos3* in WT and $Mdk^{-/-}$ collaterals 12 h after FAL as quantified by qRT-PCR. Data were normalized to the expression level of the 18S rRNA. $n = 5$ in triplicates. $^*P < 0.05$, unpaired Student's *t*-test. Data are means ± SD.

significantly smaller increase in luminal diameter after FAL (Fig. 2a and b). Moreover, the ratio of the vessel wall thickness to the luminal diameter was significantly increased in $Mdk^{-/-}$ mice (Fig. 2c). BrdU staining revealed a significantly decreased percentage of proliferating ECs in $Mdk^{-/-}$ mice, whereas there was no significant difference in the number of proliferating smooth muscle cells (SMCs) (Fig. 2d and e).

3.2. Leukocyte Domiciled MK Promotes Collateral Artery Growth

MK plasma levels prior to any surgical procedure (basal), 12 h and 24 h after FAL were below the detection range. At 3d after FAL, MK plasma level increased to 0.268 ± 0.012 ng/ml and decreased again at 7d (Fig. 3a). The *Mdk* mRNA expression levels significantly increased in collaterals 12 h and 24 h after FAL (Fig. 3b). Immunofluorescence double staining against MK and Ly-6G performed on tissue samples isolated 24 h after FAL evidenced that MK is present in perivascular neutrophils (Fig. 3c). To investigate the relevance of leukocyte derived MK, bone marrow from WT mice was transplanted into $Mdk^{-/-}$ mice ($Mdk^{-/-WT}$) and vice versa (WT $^{Mdk-/-}$). WT^{WT} and $Mdk^{-/-}$ $^{Mdk-/-}$ transplanted mice were used as control groups. Bone-marrow transplantation itself didn't affect perfusion recovery, as quantified by LDI measurements of transplanted and non-transplanted mice (Fig. S3). In comparison to $Mdk^{-/-}$ $^{Mdk-/-}$ mice, perfusion recovery was significantly increased in $Mdk^{-/-WT}$ as well as WT $^{Mdk-/-}$ mice, and reached values of WT^{WT} mice 7d after FAL (Fig. 3d). Histological analysis evidenced a significant increase of the luminal diameter of $Mdk^{-/-WT}$ mice compared to $Mdk^{-/-}$ $^{Mdk-/-}$ mice, but not in WT $^{Mdk-/-}$ mice (Fig. 3e) pointing to a relevance of bone marrow cell MK for collateral EC proliferation and hence arteriogenesis. Interestingly, MK was only detectable in plasma of WT^{WT} and WT $^{Mdk-/-}$ mice but not in $Mdk^{-/-WT}$ mice 7d after FAL (Fig. 3f).

3.3. Rescue of Arteriogenesis in $Mdk^{-/-}$ Mice

In order to elucidate the function of exogenous MK on the growth of collaterals, mice were treated with recombinant murine MK (rmMK). Treatment with rmMK normalized perfusion recovery, the luminal diameter, the ratio of the vascular wall to the luminal diameter and EC proliferation in $Mdk^{-/-}$ mice, but did not influence SMC proliferation (Fig. 4a and c–f). WT mice treated with rmMK showed significantly increased perfusion recovery 7d after FAL compared to saline treated WT mice, but the proliferation rate of vascular cells and the growth of collateral arteries were unchanged (Fig. 4a and c–f). Thus exogenous MK improved perfusion recovery in $Mdk^{-/-}$ mice via collateral growth, whereas increased perfusion recovery in WT mice was due to vasodilatation. This data suggested that MK not only promotes collateral growth, but also regulates the expression of *Nos* responsible for vasodilation. Accordingly, $Mdk^{-/-}$ and WT mice were treated with the NO-donor DETA NONOate. In $Mdk^{-/-}$ mice DETA NONOate treatment significantly increased perfusion recovery and normalized EC proliferation and collateral artery growth, whereas SMC proliferation was unaffected (Fig. 4b–f). In WT mice perfusion recovery, collateral growth as well as vascular cell proliferation was unchanged by DETA NONOate treatment (Fig. 4b–f). qRT-PCR analysis on collaterals isolated 12 h after FAL evidenced significantly decreased *Nos1* and *Nos3* expression levels in $Mdk^{-/-}$ mice compared to WT mice, while *Nos2* expression levels showed no significant differences (Fig. 4g). Since it is well described that *Nos3* deficiency is not associated with reduced collateral artery

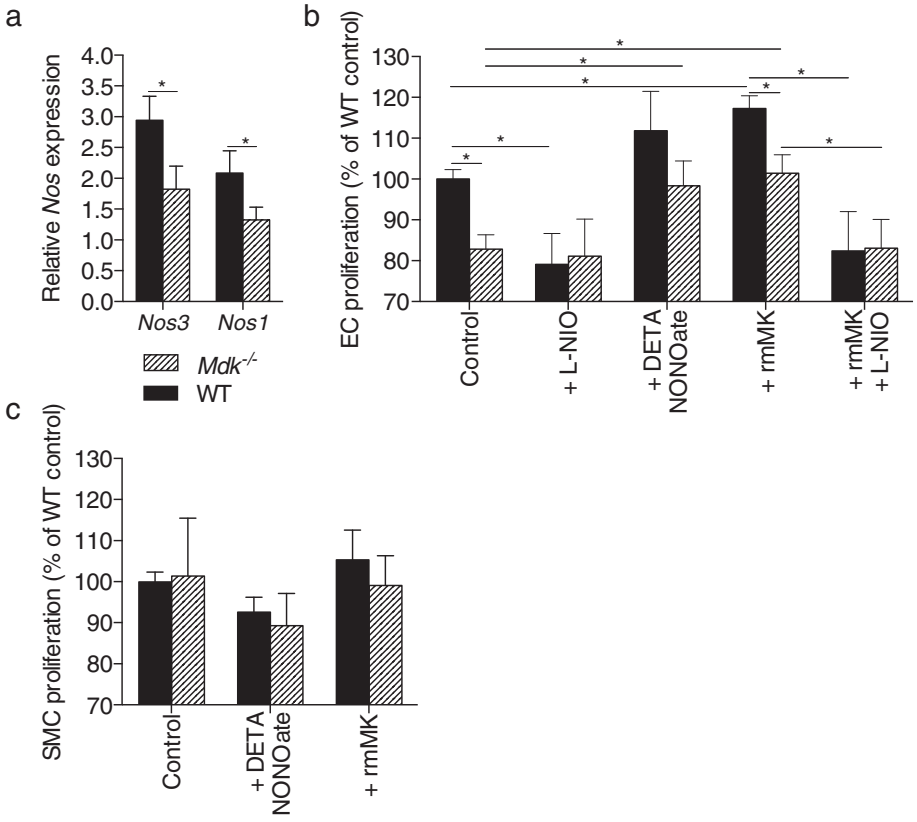

Fig. 5. In vitro analyses of vascular cells. (a) Bar graph representing the mRNA expression level of *Nos1* and *Nos3* in primary WT and $Mdk^{-/-}$ ECs. $n = 5$. *P < 0.05 unpaired Student's t-test. Data shown are means ± SD. (b, c) Proliferation rate of primary ECs and SMCs isolated from WT and $Mdk^{-/-}$ aortas as quantified by BrdU uptake. Cells were cultured for 48 h with 2%FCS in DMEM medium alone (Control), or in combination with the non-specific NOS inhibitor L-NIO (0.1 μmol/ml), DETA NONOate (50 μmol/l), rmMK (100 ng/ml), or rmMK and L-NIO. Bar graphs represent the relative proliferation rate of ECs (b) and SMCs (c). Values for WT cells cultured with 2%FCS in DMEM alone (Control) were defined as 100%. $n = 5$ in triplicates. *P < 0.05 two-way ANOVA with Bonferroni's multiple comparison test. Data are means ± SD.

growth (Troidl et al., 2010; Mees et al., 2007), but that NOS3 is relevant for proper vasodilation during arteriogenesis (Troidl et al., 2010), we asked about the relevance of *Nos1* for arteriogenesis. *Nos1*$^{-/-}$ mice did not show a reduced perfusion recovery after FAL. However, in contrast to WT and *Mdk*$^{-/-}$ mice, NO-donor treatment strikingly interfered with perfusion recovery in *Nos1*$^{-/-}$ mice (Fig. S4).

3.4. Inhibition of NOS Blocks the Proliferative Effect of rmMK on ECs In Vitro

Primary ECs of *Mdk*$^{-/-}$ showed significantly reduced basal expression levels of *Nos1* and *Nos3* (Fig. 5a) as well as a significantly reduced proliferation rate (Fig. 5b) compared to primary WT ECs. Treatment with the non-specific NOS inhibitor L-NIO significantly reduced the proliferation of WT ECs, but not of *Mdk*$^{-/-}$ ECs. Treatment with DETA NONOate as well as with rmMK increased EC proliferation of WT and *Mdk*$^{-/-}$ ECs, however, compared to WT ECs, the proliferation rate of *Mdk*$^{-/-}$ ECs was still reduced. Treatment with L-NIO abolished the positive effect of rmMK on EC proliferation in both types of cells indicating that the impact of rmMK on EC proliferation is mediated by NOS. Similar to the in vivo experiments, SMC proliferation was neither influenced by MK loss, nor by treatment with rmMK or DETA NONOate (Fig. 5c).

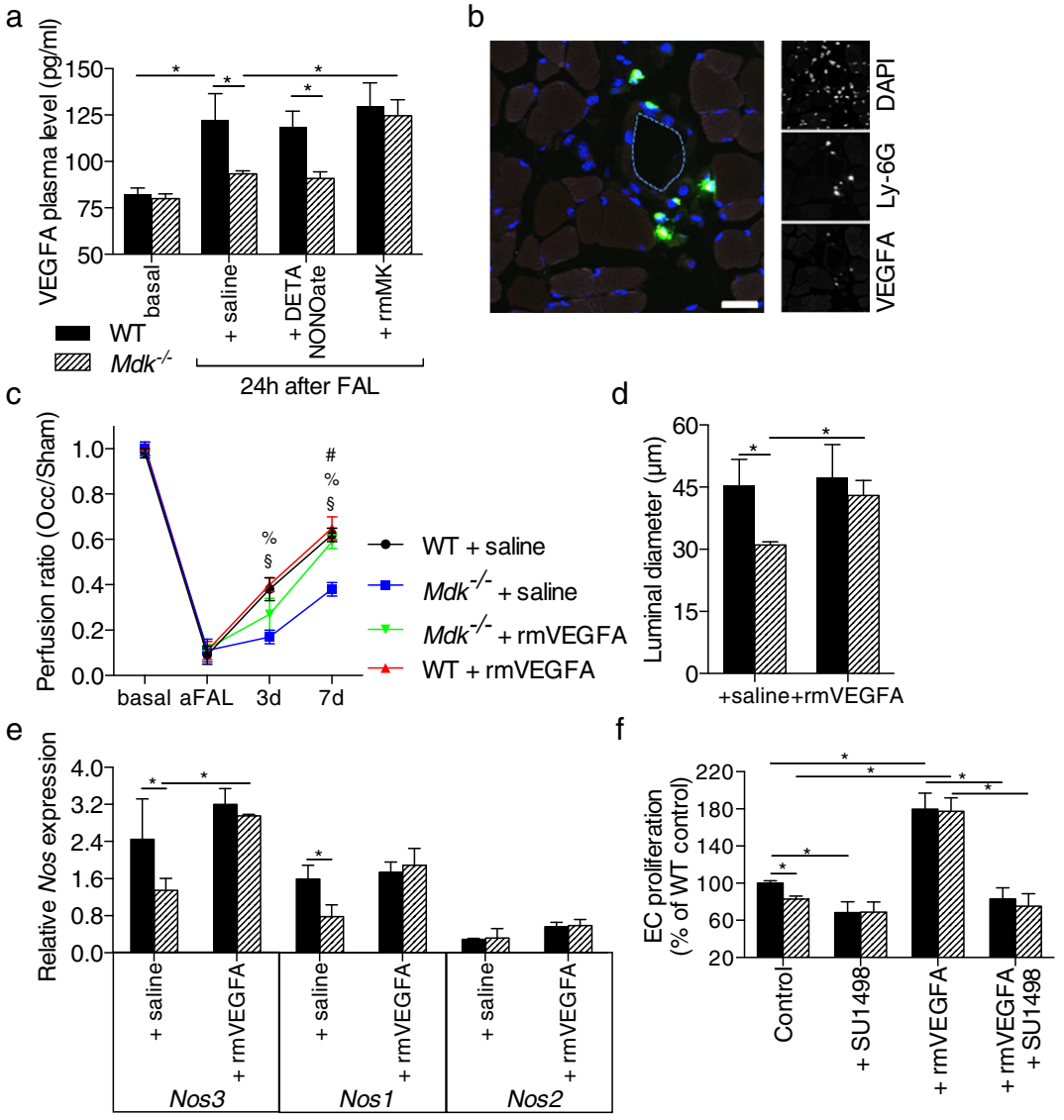

Fig. 6. Influence of VEGFA. (a) Bar graph displaying ELISA results on VEGFA plasma levels (pg/ml) in WT and *Mdk*$^{-/-}$ mice treated with saline, DETA NONOate or rmMK, respectively. Plasma was collected prior to any surgical procedure (basal) or 24 h after FAL. $n = 5$ in triplicates. *P < 0.05 one-way ANOVA with Bonferroni's multiple comparison test. (b) Triple immunofluorescence staining for VEGFA (right, lower panel), Ly-6G (right, middle panel) and DAPI (right, upper panel) 24 after FAL. Ly-6G^{+} cells in perivascular tissue stained positive for VEGFA (left panel). Blue dotted line indicates the endothelial layer of the collateral artery. Scale bar: 25 µm. (c) Line graph displaying the perfusion ratio (Occ/Sham) as measured by LDI in WT and *Mdk*$^{-/-}$ mice treated with saline or rmVEGFA. Data are show for before FAL (basal), immediately (aFAL), 3d and 7d after FAL. $n = 4$. #P < 0.05 (*Mdk*$^{-/-}$ + rmVEGFA compared with *Mdk*$^{-/-}$ + saline), §P < 0.05 (WT + rmVEGFA compared with *Mdk*$^{-/-}$ + saline), %P < 0.05 (WT + saline compared with *Mdk*$^{-/-}$ + saline), two-way ANOVA with Bonferroni's multiple comparison test. (d) Bar graph displaying the luminal diameter of collaterals in WT and *Mdk*$^{-/-}$ mice treated with saline or rmVEGFA 7d after FAL. $n = 4$. *P < 0.05, one-way ANOVA with Bonferroni's multiple comparison test. (e) Bar graph displaying the expression levels of *Nos1*, *Nos2* and *Nos3* as quantified by qRT-PCR in WT and *Mdk*$^{-/-}$ collaterals 12 h after FAL. Data were normalized to the expression level of the 18S rRNA. $n = 5$ in triplicates. *P < 0.05, two-way ANOVA with Bonferroni's multiple comparison test. (f) Bar graph representing the relative in vitro proliferation rate of WT and *Mdk*$^{-/-}$ ECs as quantified by BrdU uptake analysis. Cells were treated for 48 h with 2%FCS in DMEM medium alone (Control), or with the specific VEGFR-2 inhibitor SU1498 (100 ng/ml), with rmVEGFA (50 ng/ml), or a combination of SU1498 and rmVEGFA. Values for WT cells cultured with 2%FCS in DMEM alone (Control) were defined as 100%. $n = 5$. *P < 0.05 two-way ANOVA with Bonferroni's multiple comparison test. Data are means ± SD.

3.5. Relationship Between MK and VEGFA

Since NO has been described to induce the expression of VEGFA and vice versa (Kroll and Waltenberger, 1998; Kimura and Esumi, 2003), we investigated the plasma level of VEGFA of WT and *Mdk*$^{-/-}$ mice. Prior to any surgical procedure (basal), the plasma level of VEGFA was comparable in WT and *Mdk*$^{-/-}$ mice (Fig. 6a). 24 h after FAL the VEGFA plasma level increased significantly in WT mice, but not in *Mdk*$^{-/-}$ mice. Treatment with rmMK normalized the VEGFA plasma level of *Mdk*$^{-/-}$ mice, but showed no effect on the plasma level of WT mice. DETA NONOate treatment in contrast did not influence the plasma level of VEGFA either in WT or *Mdk*$^{-/-}$ mice. Immunohistological analysis identified neutrophils as potential source VEGFA (Fig. 6b).

7d after FAL, treatment with rmVEGFA significantly increased perfusion recovery and luminal diameter of *Mdk*$^{-/-}$ mice, however, showed no effect on WT mice (Fig. 6c and d). Moreover, treatment with rmVEGFA normalized *Nos1* and *Nos3* expression levels in collaterals of *Mdk*$^{-/-}$ mice, whereas *Nos2* expression levels were not affected either in WT or *Mdk*$^{-/-}$ mice (Fig. 6e).

Accompanying in vitro results evidenced that inhibition of VEGFR-2 by SU1498 significantly reduced the proliferation rate of primary WT ECs, but not of primary *Mdk*$^{-/-}$ ECs (Fig. 6f). Although having a broader specificity, SU1498 has been used in many experiments to block VEGFR-2 (e.g. (Greenberg and Jin, 2013)). Treatment with rmVEGFA in contrast significantly increased the proliferation rate of primary WT ECs and primary *Mdk*$^{-/-}$ ECs.

4. Discussion

In this study we identified MK as factor relevant for proper collateral EC proliferation during arteriogenesis. Our data indicate that MK regulates the bioavailability of VEGFA and modulates the differential expression of *Nos1* and *Nos3* in vascular ECs. A proposed model for the action of MK is shown in Fig. 7.

Femoral artery ligation resulted in the growth of an identical number of collateral arteries in WT and *Mdk*$^{-/-}$ mice. However, the collaterals of *Mdk*$^{-/-}$ mice showed a reduced increase of the luminal diameter with an increase of the ratio of vascular wall to luminal diameter. Thus, perfusion recovery in *Mdk*$^{-/-}$ mice was impaired due to diminished outward remodeling, although limited vasodilatation might also have contributed (see below). This kind of hypertrophic outward remodeling occurs whenever EC proliferation (intima proliferation) is compromised, while the proliferation of the media and adventitia layer is not affected (Mulvany, 1999). Indeed, our BrdU staining revealed a reduced proliferation of collateral ECs in *Mdk*$^{-/-}$ mice, while the proliferation of SMC was not negatively affected. Together, these data identify MK as cytokine relevant for collateral EC proliferation and confirm the importance of EC proliferation for the process of arteriogenesis (Moraes et al., 2013).

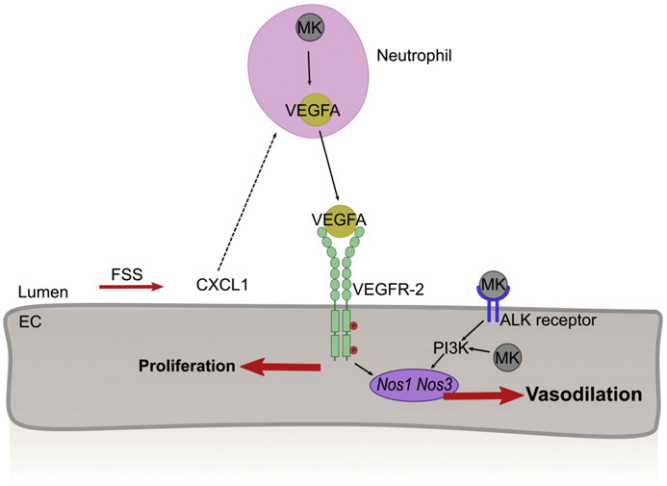

Fig. 7. Proposed model for the mechanistic function of midkine in arteriogenesis. After induction of arteriogenesis, CXCL-1, either released from platelets or EC, activates neutrophils thereby inducing MK mediated VEGFA expression and release. Upon binding to VEGFR-2, VEGFA induces the expression of *Nos1* and *Nos3*, relevant for vascular cell proliferation. However, MK also activates either directly, or indirectly by binding to ALK, PI3K resulting in NOS activation and vasodilation.

The initial phase of collateral growth relies on extravasation of leukocytes, especially neutrophils (Chillo et al., 2016). Our immunohistochemical analyses together with our bone marrow transplantation experiments identified neutrophil-domiciled midkine as relevant for arteriogenesis while non-bone marrow cell derived MK influenced perfusion recovery by increased vasodilatation. Although our data evidenced that MK is not released from leukocytes, thereby confirming previous results (Weckbach et al., 2012), we found increased plasma levels of MK 3d and 7d after FAL. FAL results – due to increased shear stress - in arteriogenesis in the upper leg, and timely delayed – due to ischemia in angiogenesis in the lower leg (Ito et al., 1997). Hypoxic ECs were recently identified as source of soluble MK in the vascular system (Weckbach et al., 2012). Accordingly it is likely that the MK observed in plasma derived from hypoxic ECs from the lower leg.

Treatment with rmMK restored perfusion recovery in *Mdk*$^{-/-}$ mice by promoting EC proliferation, while it promoted vasodilation in WT mice. These results suggested that MK might be involved in regulating NO synthases. Indeed, we found that the expression level of *Nos1* and *Nos3* was significantly reduced in ECs (but not SMCs) of *Mdk*$^{-/-}$ mice, whereas the expression level of *Nos2* was not affected. To investigate whether reduced expression of NO synthases was causative for reduced EC proliferation in *Mdk*$^{-/-}$ mice, mice were treated with the NO-donor DETA NONOate. Interestingly, DETA NONate treatment rescued arteriogenesis in *Mdk*$^{-/-}$ mice. In WT mice, however, DETA NONOate treatment did not improve arteriogenesis, and in contrast to rmMK treatment, DETA NONOate did not promote vasodilation. These data suggest that endogenous produced NO is more effective in vasodilation than an exogenous NO-donor. The receptors for MK are manifold (Weckbach et al., 2011), however, it has been shown in human umbilical vein endothelial cells (HUVECs) that stimulation with MK resulted in binding and phosphorylation of anaplastic lymphoma kinase (ALK, the receptor for PTN (pleiotrophin)) and activation of PI3K (Stoica et al., 2002). There is ample of evidence relating PI3K to *Nos1* expression (Fujibayashi et al., 2015) as well as to NOS1 (Wu et al., 2016) and NOS3 (Fisslthaler et al., 2000) activation. Together, these data suggest that ALK might have mediated the vasodilatory function of rmMK in WT mice (see also Fig. 7). However, it might be interesting to mention that intracellular MK is also capable to activate pI3K (Khan et al., 2017).

NO, particularly derived from NOS3 has been described to promote EC proliferation in vitro and angiogenesis in vivo (Fukumura et al., 2001; Cai et al., 2006; Lee et al., 1999). But studies on *Nos3*$^{-/-}$ mice suggested that NOS3 is not essential for arteriogenesis, and reduced perfusion recovery was attributed to reduced vasodilation (Troidl et al., 2010; Mees et al., 2007). *Nos1* has previously been described to be upregulated during arteriogenesis, however, its functional role remains to be elucidated (Pagel et al., 2011). Our current study showed that reperfusion recovery is not reduced in *Nos1*$^{-/-}$ mice. However, in contrast to WT or *Mdk*$^{-/-}$ mice, in which treatment with an NO-donor either did not affect (WT mice) or even promoted (*Mdk*$^{-/-}$ mice) arteriogenesis, it showed deleterious effects on perfusion recovery in *Nos1*$^{-/-}$ mice indicating that the loss of NOS1 was compensated in a manner not tolerating increased levels of NO.

Whereas NOS2 and NOS3 are mainly described to be involved in NO production, NOS1 has been more implicated in H_2O_2 generation (Capettini et al., 2010; Costa et al., 2016). However, also NOS3 can generate H_2O_2 when uncoupled (Li et al., 2002). Interestingly, NO (Cai et al., 2006) as well as H_2O_2 (Oshikawa et al., 2010; Li et al., 2015) have been shown to play a role in EC proliferation, and both NOS isoforms are

described to be capable to substitute for each other (Son et al., 1996). For example it has been show in a rodent model of cerebral aneurisma (CA) formation that expression of *Nos1* (but not *Nos2*) was upregulated in *Nos3*$^{-/-}$ mice (Aoki et al., 2011). Moreover, the incidence of CA formation was neither affected in *Nos1* nor *Nos3* deficient mice, however, increased in mice deficient for both genes (Aoki et al., 2011).

We have previously shown that VEGFA is not differentially expressed in the muscle tissue surrounding growing collaterals and is not at all expressed in collaterals (Deindl et al., 2001). Hence it was likely that the increased plasma levels of VEGFA detected 24 h after induction of arteriogenesis derived from a different source. Our immunohistological results evidenced that VEGFA is present in neutrophils. Interestingly, we have recently found that neutrophils are recruited to growing collaterals at the time point we now observed increased plasma levels of VEGFA (Chillo et al., 2016). A study on mesenchymal stem cells revealed that overexpression of MK resulted in increased mRNA expression levels of Vegfa, as well as increased amounts of VEGFA in cell supernatant (Zhao et al., 2014). Accordingly, our results suggest that expression of VEGFA in neutrophils was responsible for increased plasma levels of VEGFA in rmMK treated *Mdk*$^{-/-}$ mice, but also in WT mice showing MK expression in neutrophils.

Neutrophils are well described to play an important role in angiogenesis by supplying growth factors such as VEGFA (Gong and Koh, 2010; Scapini et al., 2004). Moreover, it has been demonstrated in a femoral artery ligation model that angiogenesis occurring in ischemic tissue is dependent on VEGFA released from neutrophils (Ohki et al., 2005). We have recently shown that angiogenesis is severely compromised in ischemic muscles of *Mdk*$^{-/-}$ mice after femoral artery ligation (Weckbach et al., 2012). Together, these data suggest that MK is relevant for the bioavailability of neutrophil-derived VEGFA not only in arteriogenesis, but also in angiogenesis.

It has been shown very elegantly by Scapini in vivo (Scapini et al., 2004) that neutrophil-derived VEGFA dependent angiogenesis is mediated by CXCL-1. Moreover, it has been demonstrated by several studies that blocking the CXCL-1 receptor CXCR2 interferes with angiogenesis (e.g. (Sukkar et al., 2008)). Platelets, of which we have shown to play an important role in arteriogenesis by activating neutrophils (Chandraratne et al., 2015; Chillo et al., 2016) are a rich source of CXCL-1. However, CXCL1, is also upregulated in ECs due to shear stress in vitro (Hagiwara et al., 1998) and in growing collaterals in vivo (Vries et al., 2015). Indeed it was recently demonstrated that blocking the CXCL-1 receptor CXCR2 interferes with arteriogenesis (Vries et al., 2015). Together these data suggest that CXCL-1 induced expression and release of VEGFA from neutrophils is mediated by MK. A proposed model for arteriogenesis is shown in Fig. 7.

Although not investigated in the present study, it is likely that at later time points of arteriogenesis (d3 and d7), where monocytes play a role (Troidl et al., 2013), VEGFA is supplied by this type of leukocyte, since also monocytes are a source of both, MK (Badila et al., 2015) and VEGFA (Ramanathan et al., 2003).

In our study, administration of rmVEGFA rescued arteriogenesis in *Mdk*$^{-/-}$ mice substantiating the relationship between MK and VEGFA. Administration of rmVEGFA to WT mice in contrast showed no effect on arteriogenesis confirming previous results (Jazwa et al., 2016). Together these data suggest that MK mediated increased bioavailability of VEGFA is necessary and sufficient to promote arteriogenesis under normal physiological conditions by regulating the expression level of *Nos1* and *Nos3* via activation of VEGFR-2. Increasing the current number of mice per group ($n = 5$ or $n = 4$) should strengthen the data in future studies.

In summary, we provide evidence that NO synthase, in particular NOS1 and NOS3 isoforms are decisive for EC proliferation in arteriogenesis. Moreover, we show that the expression of these NO synthases is mediated by MK by increasing the bioavailability of VEGFA. Together, these results might have profound impact on the treatment of patients with vascular occlusive diseases.

Funding Sources

This work was supported by the Deutsche Forschungsgemeinschaft (SFB 914/A2 to B. Walzog). J.-I. Pagel and J. Borgolte were supported by the FöFoLe Program from the LMU Munich and T. Lautz by the Lehre@LMU Program from the LMU Munich.

Conflicts of Interest

All authors declare no conflicts of interest.

Authors Contributions

TL, ML, EK, J-IP and JB performed in vivo measurements. TL performed qRT-PCR, in vitro assays and histological analyses. KT performed immunohistology, AC-M helped with qRT-PCR and in vitro analyses, and TL with writing the manuscript. BW participated in scientific discussions. DE performed experimental design, data analysis, conducted scientific direction, and wrote the manuscript.

Acknowledgments

We thank T. Muramatsu, (Department of Health Science, Aichi Gakuin University, Japan), for *Mdk*$^{-/-}$ (carrying the *Mdk*^{tm1Tmu} allele) and W. Schaper (Max Planck Institute for Heart and Lung Research, Bad Nauheim, Germany) for *Nos1*$^{-/-}$ (B6.129S4-*Nos1*^{tm1Plh}/J) mice, K. Lauber (Hospital of the University of Munich, Department of Radiation Oncology, LMU Munich, Munich, Germany) for support with bone marrow transplantations, C. Csapo and C. Winterbauer for technical assistance.

Appendix A. Supplementary data

Supplementary data to this article can be found online at https://doi.org/10.1016/j.ebiom.2017.11.020.

References

Aoki, T., Nishimura, M., Kataoka, H., Ishibashi, R., Nozaki, K., Miyamoto, S., 2011. Complementary inhibition of cerebral aneurysm formation by eNOS and nNOS. Lab. Investig. 91, 619–626.

Badila, E., Daraban, A.M., Tintea, E., Bartos, D., Alexandru, N., Georgescu, A., 2015. Midkine proteins in cardio-vascular disease. Where do we come from and where are we heading to? Eur. J. Pharmacol. 762, 464–471.

Cai, J., Jiang, W.G., Ahmed, A., Boulton, M., 2006. Vascular endothelial growth factor-induced endothelial cell proliferation is regulated by interaction between VEGFR-2, SH-PTP1 and eNOS. Microvasc. Res. 71, 20–31.

Capettini, L.S., Cortes, S.F., Lemos, V.S., 2010. Relative contribution of eNOS and nNOS to endothelium-dependent vasodilation in the mouse aorta. Eur. J. Pharmacol. 643, 260–266.

Chandraratne, S., VON Bruehl, M.L., Pagel, J.I., Stark, K., Kleinert, E., Konrad, I., Farschtschi, S., Coletti, R., Gartner, F., Chillo, O., Legate, K.R., Lorenz, M., Rutkowski, S., Caballero-Martinez, A., Starke, R., Tirniceriu, A., Pauleikhoff, L., Fischer, S., Assmann, G., Mueller-Hoecker, J., Ware, J., Nieswandt, B., Schaper, W., Schulz, C., Deindl, E., Massberg, S., 2015. Critical role of platelet glycoprotein ibα in arterial remodeling. Arterioscler. Thromb. Vasc. Biol. 35, 589–597.

Chillo, O., Kleinert, E.C., Lautz, T., Lasch, M., Pagel, J.I., Heun, Y., Troidl, K., Fischer, S., Caballero-Martinez, A., Mauer, A., Kurz, A.R., Assmann, G., Rehberg, M., Kanse, S.M., Nieswandt, B., Walzog, B., Reichel, C.A., Mannell, H., Preissner, K.T., Deindl, E., 2016. Perivascular mast cells govern shear stress-induced arteriogenesis by orchestrating leukocyte function. Cell Rep. 16, 2197–2207.

Choudhuri, R., Zhang, H.T., Donnini, S., Ziche, M., Bicknell, R., 1997. An angiogenic role for the neurokines midkine and pleiotrophin in tumorigenesis. Cancer Res. 57, 1814–1819.

Costa, E.D., Rezende, B.A., Cortes, S.F., Lemos, V.S., 2016. Neuronal nitric oxide synthase in vascular physiology and diseases. Front. Physiol. 7, 206.

Deindl, E., Buschmann, I., Hoefer, I.E., Podzuweit, T., Boengler, K., Vogel, S., VAN Royen, N., Fernandez, B., Schaper, W., 2001. Role of ischemia and hypoxia-inducible genes in arteriogenesis after femoral artery occlusion in the rabbit. Circ. Res. 89, 779–786.

Fisslthaler, B., Dimmeler, S., Hermann, C., Busse, R., Fleming, I., 2000. Phosphorylation and activation of the endothelial nitric oxide synthase by fluid shear stress. Acta Physiol. Scand. 168, 81–88.

Fujibayashi, T., Kurauchi, Y., Hisatsune, A., Seki, T., Shudo, K., Katsuki, H., 2015. Mitogen-activated protein kinases regulate expression of neuronal nitric oxide synthase and

neurite outgrowth via non-classical retinoic acid receptor signaling in human neuroblastoma SH-SY5Y cells. J. Pharmacol. Sci. 129, 119–126.
Fukumura, D., Gohongi, T., Kadambi, A., Izumi, Y., Ang, J., Yun, C.O., Buerk, D.G., Huang, P.L., Jain, R.K., 2001. Predominant role of endothelial nitric oxide synthase in vascular endothelial growth factor-induced angiogenesis and vascular permeability. Proc. Natl. Acad. Sci. U. S. A. 98, 2604–2609.
Gong, Y., Koh, D.R., 2010. Neutrophils promote inflammatory angiogenesis via release of preformed VEGF in an in vivo corneal model. Cell Tissue Res. 339, 437–448.
Greenberg, D.A., Jin, K., 2013. Vascular endothelial growth factors (VEGFs) and stroke. Cell. Mol. Life Sci. 70, 1753–1761.
Hagiwara, H., Mitsumata, M., Yamane, T., Jin, X., Yoshida, Y., 1998. Laminar shear stress-induced GRO mRNA and protein expression in endothelial cells. Circulation 98, 2584–2590.
Hannas, B.R., Das, P.C., Li, H. & Leblanc, G. A., 2010. Intracellular conversion of environmental nitrate and nitrite to nitric oxide with resulting developmental toxicity to the crustacean *Daphnia magna*. PLoS One 5, e12453.
Hayashi, K., Banno, H., Kadomatsu, K., Takei, Y., Komori, K., Muramatsu, T., 2005. Antisense oligodeoxyribonucleotide as to the growth factor midkine suppresses neointima formation induced by balloon injury. Am. J. Physiol. Heart Circ. Physiol. 288, H2203–9.
Horiba, M., Kadomatsu, K., Nakamura, E., Muramatsu, H., Ikematsu, S., Sakuma, S., Hayashi, K., Yuzawa, Y., Matsuo, S., Kuzuya, M., Kaname, T., Hirai, M., Saito, H., Muramatsu, T., 2000. Neointima formation in a restenosis model is suppressed in midkine-deficient mice. J. Clin. Invest. 105, 489–495.
Huang, P.L., Dawson, T.M., Bredt, D.S., Snyder, S.H., Fishman, M.C., 1993. Targeted disruption of the neuronal nitric oxide synthase gene. Cell 75, 1273–1286.
Ito, W.D., Arras, M., Scholz, D., Winkler, B., Htun, P., Schaper, W., 1997. Angiogenesis but not collateral growth is associated with ischemia after femoral artery occlusion. Am. J. Phys. 273, H1255–65.
Jazwa, A., Florczyk, U., Grochot-Przeczek, A., Krist, B., Loboda, A., Jozkowicz, A., Dulak, J., 2016. Limb ischemia and vessel regeneration: is there a role for VEGF? Vasc. Pharmacol. 86, 18–30.
Kadomatsu, K., Huang, R.P., Suganuma, T., Murata, F., Muramatsu, T., 1990. A retinoic acid responsive gene MK found in the teratocarcinoma system is expressed in spatially and temporally controlled manner during mouse embryogenesis. J. Cell Biol. 110, 607–616.
Khan, N., Binder, L., Pantakani, D.V.K., Asif, A.R., 2017. MPA modulates tight junctions' permeability via midkine/PI3K pathway in caco-2 cells: a possible mechanism of leak-flux diarrhea in organ transplanted patients. Front. Physiol. 8, 438.
Kimura, H., Esumi, H., 2003. Reciprocal regulation between nitric oxide and vascular endothelial growth factor in angiogenesis. Acta Biochim. Pol. 50, 49–59.
Kobayashi, M., Inoue, K., Warabi, E., Minami, T., Kodama, T., 2005. A simple method of isolating mouse aortic endothelial cells. J. Atheroscler. Thromb. 12, 138–142.
Kroll, J., Waltenberger, J., 1998. VEGF-A induces expression of eNOS and iNOS in endothelial cells via VEGF receptor-2 (KDR). Biochem. Biophys. Res. Commun. 252, 743–746.
Kumar, D., Branch, B.G., Pattillo, C.B., Hood, J., Thoma, S., Simpson, S., Illum, S., Arora, N., Chidlow Jr., J.H., Langston, W., Teng, X., Lefer, D.J., Patel, R.P., Kevil, C.G., 2008. Chronic sodium nitrite therapy augments ischemia-induced angiogenesis and arteriogenesis. Proc. Natl. Acad. Sci. U. S. A. 105, 7540–7545.
Lee, P.C., Salyapongse, A.N., Bragdon, G.A., Shears II, L.L., Watkins, S.C., Edington, H.D., Billiar, T.R., 1999. Impaired wound healing and angiogenesis in eNOS-deficient mice. Am. J. Phys. 277, H1600–8.
Li, H., Wallerath, T., Munzel, T., Forstermann, U., 2002. Regulation of endothelial-type NO synthase expression in pathophysiology and in response to drugs. Nitric Oxide 7, 149–164.
Li, J., Wang, J.J., Zhang, S.X., 2015. NADPH oxidase 4-derived H2O2 promotes aberrant retinal neovascularization via activation of VEGF receptor 2 pathway in oxygen-induced retinopathy. J. Diabetes Res. 2015, 963289.
Mees, B., Wagner, S., Ninci, E., Tribulova, S., Martin, S., van Haperen, R., Kostin, S., Heil, M., DE Crom, R., Schaper, W., 2007. Endothelial nitric oxide synthase activity is essential for vasodilation during blood flow recovery but not for arteriogenesis. Arterioscler. Thromb. Vasc. Biol. 27, 1926–1933.
Moraes, F., Paye, J., Mac Gabhann, F., Zhuang, Z.W., Zhang, J., Lanahan, A.A., Simons, M., 2013. Endothelial cell-dependent regulation of arteriogenesis. Circ. Res. 113, 1076–1086.
Mulvany, M.J., 1999. Vascular remodelling of resistance vessels: can we define this? Cardiovasc. Res. 41, 9–13.
Muramaki, M., Miyake, H., Hara, I., Kamidono, S., 2003. Introduction of midkine gene into human bladder cancer cells enhances their malignant phenotype but increases their sensitivity to antiangiogenic therapy. Clin. Cancer Res. 9, 5152–5160.
Nakamura, E., Kadomatsu, K., Yuasa, S., Muramatsu, H., Mamiya, T., Nabeshima, T., Fan, Q.W., Ishiguro, K., Igakura, T., Matsubara, S., Kaname, T., Horiba, M., Saito, H., Muramatsu, T., 1998. Disruption of the midkine gene (Mdk) resulted in altered expression of a calcium binding protein in the hippocampus of infant mice and their abnormal behaviour. Genes Cells 3, 811–822.
Narita, H., Chen, S., Komori, K., Kadomatsu, K., 2008. Midkine is expressed by infiltrating macrophages in in-stent restenosis in hypercholesterolemic rabbits. J. Vasc. Surg. 47, 1322–1329.
Ohki, Y., Heissig, B., Sato, Y., Akiyama, H., Zhu, Z., Hicklin, D.J., Shimada, K., Ogawa, H., Daida, H., Hattori, K., Ohsaka, A., 2005. Granulocyte colony-stimulating factor promotes neovascularization by releasing vascular endothelial growth factor from neutrophils. FASEB J. 19, 2005–2007.
Oshikawa, J., Urao, N., Kim, H.W., Kaplan, N., Razvi, M., Mckinney, R., Poole, L.B., Fukai, T., Ushio-Fukai, M., 2010. Extracellular SOD-derived H_2O_2 promotes VEGF signaling in caveolae/lipid rafts and post-ischemic angiogenesis in mice. PLoS One 5, e10189.
Pagel, J.I., Borgolte, J., Hoefer, I., Fernandez, B., Schaper, W., Deindl, E., 2011. Involvement of neuronal NO synthase in collateral artery growth. Indian J. Biochem. Biophys. 48, 270–274.
Ramanathan, M., Giladi, A., Leibovich, S.J., 2003. Regulation of vascular endothelial growth factor gene expression in murine macrophages by nitric oxide and hypoxia. Exp. Biol. Med. (Maywood) 228, 697–705.
Scapini, P., Morini, M., Tecchio, C., Minghelli, S., DI Carlo, E., Tanghetti, E., Albini, A., Lowell, C., Berton, G., Noonan, D.M., Cassatella, M.A., 2004. CXCL1/macrophage inflammatory protein-2-induced angiogenesis in vivo is mediated by neutrophil-derived vascular endothelial growth factor-A. J. Immunol. 172, 5034–5040.
Son, H., Hawkins, R.D., Martin, K., Kiebler, M., Huang, P.L., Fishman, M.C., Kandel, E.R., 1996. Long-term potentiation is reduced in mice that are doubly mutant in endothelial and neuronal nitric oxide synthase. Cell 87, 1015–1023.
Stoica, G.E., Kuo, A., Powers, C., Bowden, E.T., Sale, E.B., Riegel, A.T., Wellstein, A., 2002. Midkine binds to anaplastic lymphoma kinase (ALK) and acts as a growth factor for different cell types. J. Biol. Chem. 277, 35990–35998.
Sukkar, A., Jenkins, J., Sanchez, J., Wagner, E.M., 2008. Inhibition of CXCR2 attenuates bronchial angiogenesis in the ischemic rat lung. J. Appl. Physiol. 1985 (104), 1470–1475.
Takada, T., Toriyama, K., Muramatsu, H., Song, X.J., Torii, S., Muramatsu, T., 1997. Midkine, a retinoic acid-inducible heparin-binding cytokine in inflammatory responses: chemotactic activity to neutrophils and association with inflammatory synovitis. J. Biochem. 122, 453–458.
Troidl, K., Tribulova, S., Cai, W.J., Ruding, I., Apfelbeck, H., Schierling, W., Troidl, C., Schmitz-Rixen, T., Schaper, W., 2010. Effects of endogenous nitric oxide and of DETA NONOate in arteriogenesis. J. Cardiovasc. Pharmacol. 55, 153–160.
Troidl, C., Jung, G., Troidl, K., Hoffmann, J., Mollmann, H., Nef, H., Schaper, W., Hamm, C.W., Schmitz-Rixen, T., 2013. The temporal and spatial distribution of macrophage subpopulations during arteriogenesis. Curr. Vasc. Pharmacol. 11, 5–12.
Tzima, E., Irani-Tehrani, M., Kiosses, W.B., Dejana, E., Schultz, D.A., Engelhardt, B., Cao, G., Delisser, H., Schwartz, M.A., 2005. A mechanosensory complex that mediates the endothelial cell response to fluid shear stress. Nature 437, 426–431.
Vries, M.H., Wagenaar, A., Verbruggen, S.E., Molin, D.G., Dijkgraaf, I., Hackeng, T.H., Post, M.J., 2015. CXCL1 promotes arteriogenesis through enhanced monocyte recruitment into the peri-collateral space. Angiogenesis 18, 163–171.
Weckbach, L.T., Muramatsu, T., Walzog, B., 2011. Midkine in inflammation. ScientificWorldJournal 11, 2491–2505.
Weckbach, L.T., Groesser, L., Borgolte, J., Pagel, J.I., Pogoda, F., Schymeinsky, J., Muller-Hocker, J., Shakibaei, M., Muramatsu, T., Deindl, E., Walzog, B., 2012. Midkine acts as proangiogenic cytokine in hypoxia-induced angiogenesis. Am. J. Physiol. Heart Circ. Physiol. 303, H429–38.
Weckbach, L.T., Gola, A., Winkelmann, M., Jakob, S.M., Groesser, L., Borgolte, J., Pogoda, F., Pick, R., Pruenster, M., Muller-Hocker, J., Deindl, E., Sperandio, M., Walzog, B., 2014. The cytokine midkine supports neutrophil trafficking during acute inflammation by promoting adhesion via beta2 integrins (CD11/CD18). Blood 123, 1887–1896.
Wu, Z.T., Ren, C.Z., Yang, Y.H., Zhang, R.W., Sun, J.C., Wang, Y.K., Su, D.F., Wang, W.Z., 2016. The PI3K signaling-mediated nitric oxide contributes to cardiovascular effects of angiotensin-(1-7) in the nucleus tractus solitarii of rats. Nitric Oxide 52, 56–65.
Zhao, S.L., Zhang, Y.J., Li, M.H., Zhang, X.L., Chen, S.L., 2014. Mesenchymal stem cells with overexpression of midkine enhance cell survival and attenuate cardiac dysfunction in a rat model of myocardial infarction. Stem Cell Res Ther 5, 37.